Molecular Crystals and Liquid Crystals

Publication details, including instructions for authors and subscription information:
http://www.tandfonline.com/loi/gmcl20

Numerical and Experimental Studies of Liquid Crystal Lens with Stacked Structure of Two Liquid Crystal Layers

Bin Wang [a], Mao Ye [a], Marenori Kawamura [a], Rumiko Yamaguchi [a] & Susumu Sato [a]

[a] Department of Electrical and Electronic Engineering, Akita University, Akita, Japan

Version of record first published: 22 Sep 2010

To cite this article: Bin Wang, Mao Ye, Marenori Kawamura, Rumiko Yamaguchi & Susumu Sato (2008): Numerical and Experimental Studies of Liquid Crystal Lens with Stacked Structure of Two Liquid Crystal Layers, Molecular Crystals and Liquid Crystals, 480:1, 36-43

To link to this article: http://dx.doi.org/10.1080/15421400701821457

Mol. Cryst. Liq. Cryst., Vol. 480, pp. 36–43, 2008

ISSN: 1542-1406 print/1563-5287 online
DOI: 10.1080/15421400701821457

Taylor & Francis
Taylor & Francis Group

Numerical and Experimental Studies of Liquid Crystal Lens with Stacked Structure of Two Liquid Crystal Layers

Bin Wang, Mao Ye, Marenori Kawamura, Rumiko Yamaguchi, Susumu Sato
Department of Electrical and Electronic Engineering, Akita University, Akita, Japan

A liquid crystal lens with stacked structure of two liquid crystal layers is prepared and its numerical and experimental studies are reported. The two liquid crystal layers work together to form an optical lens. The electric field, the molecular reorientation, and the phase retardation induced on an incident light wave are calculated. Experimental results are compared with the calculations. The driving method avoiding disclination occurring is discussed.

Keywords: disclination line; liquid crystal lens; stacked structure

INTRODUCTION

Liquid crystal (LC) lens attracts a lot of research interest, and various kinds of lens structures have been proposed [1–10]. Recently, a two-voltage-driving LC lens of much improved properties has been reported [11]. Its focus is variable in a wide range, and over the entire focus range the lens preserves its optical quality. By using the driving method, an LC lens with a stacked structure of thin LC layers has been fabricated successfully [12], and not only fast operation but also wide focus range are realized. In this article, numerical and experimental studies on the LC lens is reported. The electrical field, the director reorientation, and the phase retardation induced on an incident light wave are calculated. Experimental results are compared with the calculation. The driving method avoiding disclination occurring is discussed.

Address correspondence to Marenori Kawamura, Department of Electrical and Electronic Engineering, Akita University, 1-1 Tegatagakuen-cho, Akita 010-8502, Japan. E-mail: kawamura@ipc.akita-u.ac.jp

MOLECULAR REORIENTATION

The structure of the LC lens is shown in Figure 1. There are two 20-μm LC (Merck E44) layers in the cell. One (LC layer 1) is between glass substrates 1 and 2, and the other (LC layer 2) between glass substrates 2 and 3. The surfaces of the glass substrates confining the LC layers are coated with polyimide (JSR Optmer AL 1254) films and are rubbed with cloth and the LC directors initially align homogeneously. The LC directors in the two layers pre-tilt to opposite directions with a pre-tilt angle θ_0 of approximate 2.5°. The thicknesses of substrates 2 and 3 influence the lens properties and are 70 and 500 μm, respectively. There are two transparent indium tin oxide (ITO) electrodes sputtered on substrates 1 and 4, and one aluminum electrode (Al) with a circular hole of 2.5-mm diameter in the center coated on substrate 3, in the cell. The air gap between substrates 3 and 4 is 20-μm thickness. Two voltages of 1 kHz frequency V_o across the Al electrode and V_c across the two ITO electrodes are applied. $V_o = 150\,V_{rms}$ acts as a biases voltage remaining unchanged, and V_c varies from 40 to $90\,V_{rms}$ to tune the lens properties.

Voltages V_o and V_c build up a spatially inhomogeneous electric field $\boldsymbol{E}$ in the LC layers, resulting in a spatially nonuniform director reorientation. At the equilibrium state, the orientation of the LC directors $\boldsymbol{n} = (n_x, n_y, n_z)$ should obey the Euler equations $-\partial f/\partial n_\alpha + \partial[\partial f/\partial(\partial n_\alpha/\partial\beta)]/\partial\beta = 0$ so that the total free energy of the LC cell is the

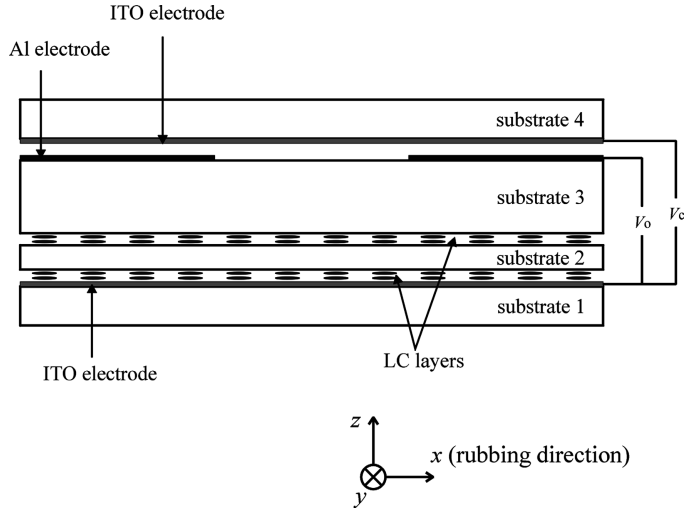

FIGURE 1 Structure of LC lens.

minimum [13]. In the equations, α and β denote the x, y, or, z components, and $f = (1/2)[K_{11}(\nabla \cdot \boldsymbol{n})^2 + K_{22}(\boldsymbol{n} \cdot \nabla \times \boldsymbol{n})^2 + K_{33}(\boldsymbol{n} \times \nabla \times \boldsymbol{n})^2] - (1/8\pi)(\varepsilon_{LC} \cdot \boldsymbol{E}) \cdot \boldsymbol{E}$ is the free energy density [14], where K_{11}, K_{22}, and K_{33} are, respectively, the splay, twist, and bend elastic constants of the LC. The electric field $\boldsymbol{E} = -\nabla V$, where V denotes the potential, and the dielectric constant of the LC $\varepsilon_{LC}^{\alpha\beta} = \varepsilon_\perp \delta_{\alpha\beta} + (\varepsilon_{||} - \varepsilon_\perp)\boldsymbol{n}_\alpha \boldsymbol{n}_\beta$, where $\varepsilon_{||}$ and $\varepsilon_\perp$ are the dielectric constants of the LC parallel and perpendicular to the local LC directors, respectively. The electric field obeys the Maxwell's equation $\nabla \cdot (\varepsilon \cdot \boldsymbol{E}) = 0$, where the dielectric constant ε is that of the glass ε_{g} in the glass, or that of the LC $\varepsilon_{\mathrm{LC}}$ in the LC. The

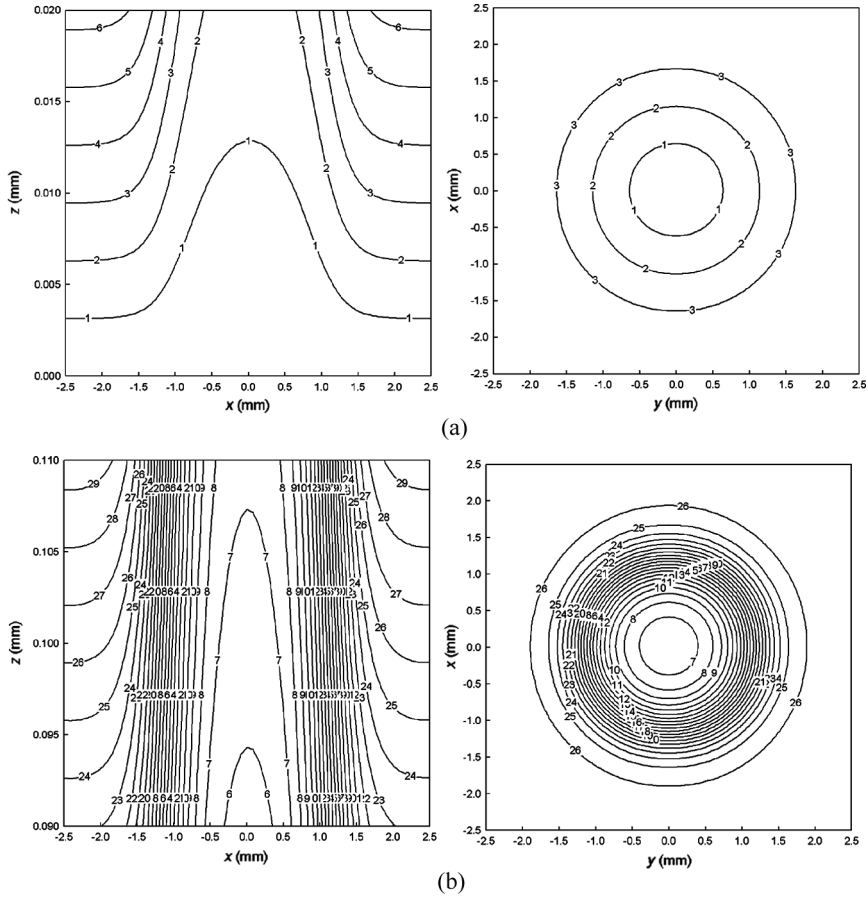

FIGURE 2 Equipotential lines in LC layers at $V_{\mathrm{c}} = 40\,\mathrm{V_{rms}}$: (a) in the planes of y = 0 and $z = 10\,\mu\mathrm{m}$ in LC layer 1, (b) in the planes of $y = 0$ and $z = 100\,\mu\mathrm{m}$ in LC layer 2.

equations for the LC directors $\boldsymbol{n}$ and the electric field $\boldsymbol{E}$ are integrated numerically [15,16]. The physical parameters of E44 used in the calculation are $\varepsilon_{||} = 22.0$, $\varepsilon_{\perp} = 5.2$, $K_{11} = 15.5 \times 10^{-7}$ dyne, $K_{22} = 13.0 \times 10^{-7}$ dyne, and $K_{33} = 28.0 \times 10^{-7}$ dyne. The dielectric constant of glass substrate is 6.9. The origin of the coordinate system is located in the center of the lower ITO electrode.

Figure 2 shows the calculated results of the distribution of electric field in the LC layers before the director reorientation. In both LC layers 1 (Fig. 2(a)) and 2 (Fig. 2(b)), the electric field is nearly axially symmetrical and decreases gradually from the boundary to the center. The gradient of $\boldsymbol{E}$ is greater in LC layer 2 than in LC layer 1. And there is a larger horizontal component of $\boldsymbol{E}$ in LC layer 2 than in LC layer 1.

The local LC directors are tilted up by the electric torque proportional to $\boldsymbol{E}^2$ to align with the electric field until the electric torque is balanced by the elastic one exerted by the surrounding LC directors. Figure 3 shows the tilt angle θ of the LC directors in the planes $z = 10\,\mu\text{m}$ (in the middle of LC layer 1) (Fig. 3(a)) and $z = 100\,\mu\text{m}$ (in the middle of LC layer 2) (Fig. 3(b)). As the local tilt angle θ generally increases with the local electric field $\boldsymbol{E}$, it decreases gradually from the boundary to the center. Due to the larger inclination of $\boldsymbol{E}$ in LC layer 2 as shown in Figure 2(b), the dissymmetrical property of θ along the rubbing direction (parallel with the x-axis) is more obvious in LC layer 2 than in LC layer 1.

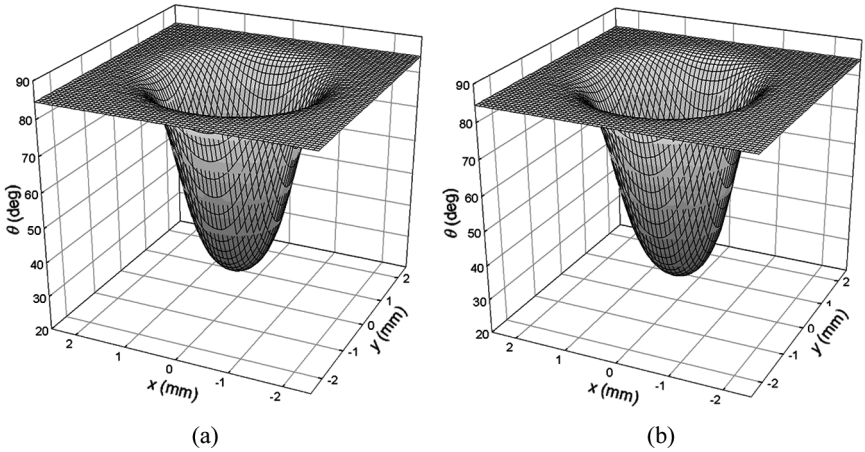

FIGURE 3 Tilt angle of LC directors in: (a) $z = 10\,\mu\text{m}$ and (b) $z = 100\,\mu\text{m}$ planes.

OPTICAL PROPERTIES

An incident plane light wave polarized in the rubbing direction, that is, an extraordinary wave, experiences a refractive index $n_e(\theta) = n_o n_e/(n_e^2 \sin^2\theta + n_o^2 \cos^2\theta)^{1/2}$, where n_o and n_e are the ordinary and extraordinary refractive indices of the LC, respectively. In the experiment, a laser beam of 633 nm wavelength from a He-Ne laser is used to investigate the lens properties. At room temperature of approximately 25°C, the refractive indices are $n_o = 1.523$ and $n_e = 1.775$. $n_e(\theta)$ then takes a profile that is the largest at the center and decreased gradually with distance from the center. The spatial variance of the refractive index results in a spatially inhomogeneous phase retardation $\phi = (2\pi/\lambda)\left[\int_0^{t_1} n_e(\theta)\mathrm{d}z + \int_{t_1+t_{g1}}^{t_1+t_{g1}+t_2} n_e(\theta)\mathrm{d}z\right]$, where t_1, t_{g1} and t_2 are the thicknesses of LC layer 1, substrate 2 and LC layer 2, respectively, and the wavefront of the incident light beam then turns from plane to a bell-like profile.

The properties of the LC lens are measured by interference method. Figure 4(a) shows the interference pattern at voltages $V_o = 150\,V_{rms}$ and $V_c = 40\,V_{rms}$. The phase difference between adjacent interference fringes is 2π. Figure 4(b) shows the calculated result of the interference fringes. The circular fringes suggest the axially symmetry of the lens properties. The slight dissymmetry of the fringes along the rubbing direction can be seen. The phase retardation profiles measured along the x-axis (rubbing direction) and the y-axis are shown in Figure 5. The dots represent measurements, the solid lines the calculations, and the dashes lines quadratic fittings. It can be seen that the phase profiles of the light wave are very close to the phase transformation of a lens, and the LC cell acts as an optical lens; phase

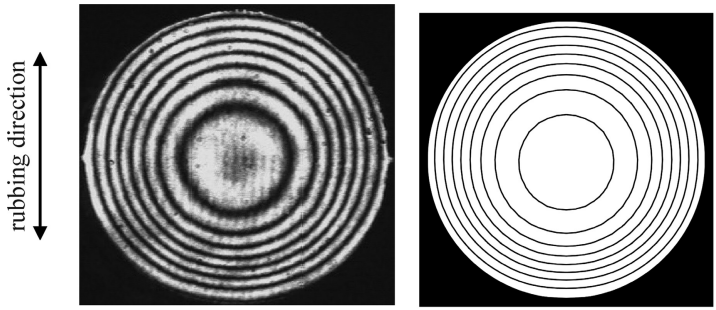

FIGURE 4 Interference fringes at $V_c = 40\,V_{rms}$: (a) experiment, (b) calculation.

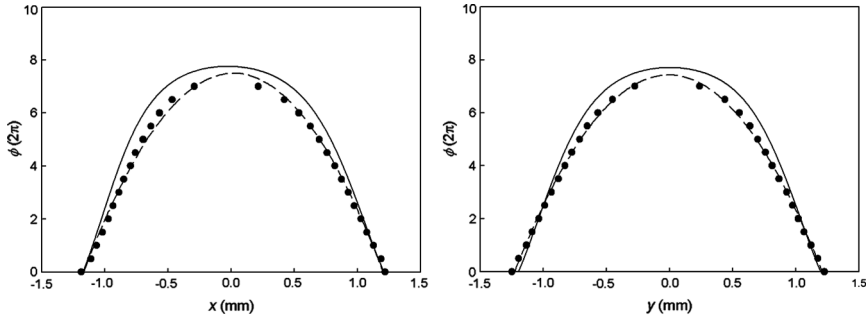

FIGURE 5 Phase profile at $V_c = 40\,V_{rms}$ measured along x-axis (a) and y-axis (b).

retardation takes a lens-like shape of $k\rho^2/(2f)$, where $\rho = (x^2 + y^2)^{1/2}$ is the radial position, $k = 2\pi/\lambda$ the wave number of the light wave, and f the focal length [17]. The lens power $P = 1/f$ [18] at various V_c is shown in Figure 6, the dots represent measurements and the curve the calculation. P decreases monotonically with V_c in a wide range.

DISCLINATION

If V_o and V_c are applied simultaneously on the cell, disclination lines may occur in the LC layers, in particular in LC layer 2, due to the

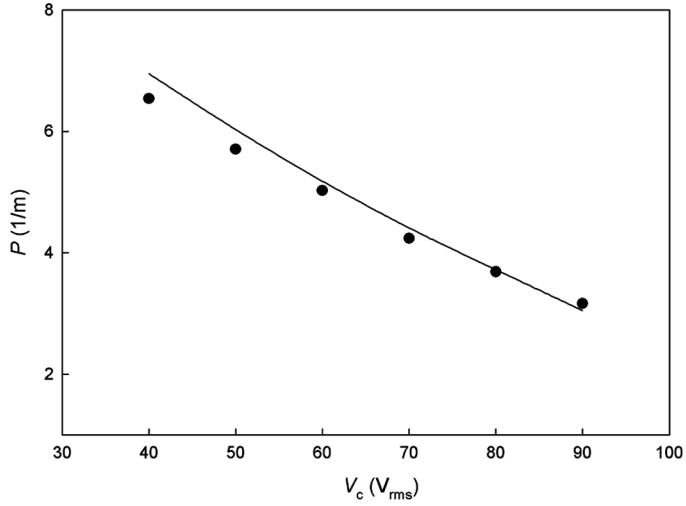

FIGURE 6 Lens power at various values of V_c.

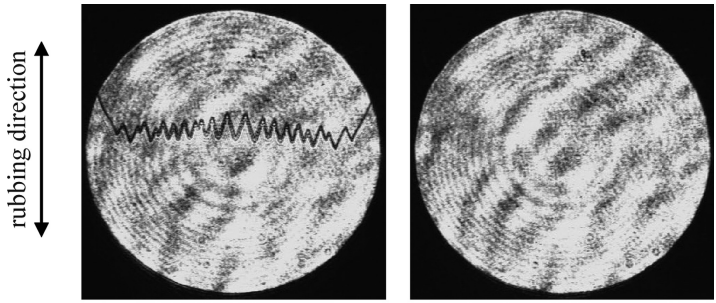

FIGURE 7 LC cell observed when (a) $V_o = 150\,V_{rms}$ and $V_c = 40\,V_{rms}$ are applied simultaneously. (b) $V_o = V_c = 150\,V_{rms}$ are applied at first and then V_c is switched from 150 to $40\,V_{rms}$.

inclinations of the electric field. Figure 7(a) shows the observed disclination line when $V_o = 150\,V_{rms}$ and $V_c = 40\,V_{rms}$ are applied directly on the cell. The disclination is the boundary of the domains of reverse tilt of the LC directors. To avoid the reverse tilt, the cell is driven by applying voltages $V_c = V_o = 150\,V_{rms}$ on the cell at first, and then switching V_c from 150 to the required value of $40\,V_{rms}$. In this way, disclination line does not appear (Fig. 7(b)).

CONCLUSIONS

The electric field gradient is greater in LC layer 2 than in LC layer 1, and there is larger horizontal component of the electric field in the LC layer 2. Consequently, the dissymmetrical property along the rubbing direction is more obvious in LC layer 2, and it is easier for disclination to occur in LC layer 2. Numerical and experimental studies on the lens are presented. The calculated properties are close to the measurements.

REFERENCES

[1] Sato, S. (1979). *Jpn. J. Appl. Phys.*, *18*, 1679.
[2] Kowel, S. T., Cleverly, D. S., & Kornreich, P. G. (1984). *Appl. Opt.*, *23*, 278.
[3] Nose, T. & Sato, S. (1989). *Liq. Cryst.*, *5*, 1425.
[4] Nose, T., Masuda, S., & Sato, S. (1991). *Jpn. J. Appl. Phys.*, *30*, L2110.
[5] Riza, N. A. & DeJule, M. C. (1994). *Opt. Lett.*, *19*, 1013.
[6] Naumov, F., Loktev, M. Yu., Guralnik, I. R., & Vdovin, G. (1998). *Opt. Lett.*, *23*, 992.
[7] Ye, M. & Sato, S. (2002). *Jpn. J. Appl. Phys.*, *41*, L571.

[8] Wang, B., Ye, M., Honma, M., Nose, T., & Sato, S. (2002). *Jpn. J. Appl. Phys.*, *41*, L1232.
[9] Ren, H. & Wu, S. T. (2003). *Appl. Phys. Lett.*, *82*, 22.
[10] Wang, B., Ye, M., & Sato, S. (2004). *Appl. Opt.*, *43*, 3420.
[11] Ye, M., Wang, B., & Sato, S. (2004). *Appl. Opt.*, *43*, 6407.
[12] Wang, B., Ye, M., & Sato, S. (2005). *Opt. Commun.*, *250*, 266.
[13] Arnold, V. I. (1978). *Mathematical Methods of Classical Mechanics*, Springer-Verlag, New York, Inc.: New York.
[14] de Gennes, P. G. (1974). *The Physics of Liquid Crystals*, Oxford Univ. Press: London.
[15] Mori, H., Gartland, E. C., Jr., Kelly, J. R., & Bos, P. J. (1999). *Jpn. J. Appl. Phys.*, *38*, 135.
[16] Ye, M. & Sato, S. (2001). *Jpn. J. Appl. Phys.*, *40*, 6012.
[17] Goodman, J. W. (1968). *Introduction to Fourier Optics*, McGraw-Hill Book Company: San Francisco.
[18] Born, M. & Wolf, E. (1975). *Principles of Optics*, Pergamon Press: Oxford.